

# Chapter 28

## Hamiltonian Chaos: Theory

We imagine starting with an integrable Hamiltonian with  $N$  degrees of freedom, and then adding a nonintegrable Hamiltonian perturbation

$$H = H_0(\vec{I}) + \varepsilon H_1(\vec{\theta}, \vec{I}) \quad (28.1)$$

where  $H_0$  gives motion on an  $N$ -torus with frequencies  $\dot{\theta}_i = \omega_{0,i} = \partial H_0 / \partial I_i$ .

### 28.1 KAM Theory

If the unperturbed system satisfies certain “non-degeneracy” conditions (e.g. a nonzero determinant  $|\partial \vec{\omega}_0 / \partial \vec{I}|$ ) then for a sufficiently small perturbation most invariant tori do not vanish but are only slightly deformed, so that in phase space there are invariant tori densely filled with quasiperiodic curves winding around them. Here “most” means that the measure of their complement is small and goes to zero with the size of the perturbation. The tori that survive are the ones that are “sufficiently irrational”. Conditions on which irrational tori survive take the form of “diophantine conditions” on the unperturbed frequencies  $\vec{\omega}_0$ . An expression  $\vec{\omega} \cdot \vec{k} = 0$  with  $\vec{k}$  a vector of integers gives a rational relationship between the frequencies  $\omega_i$ : these tori will be destroyed. For irrational frequencies this condition will not be satisfied for any  $\vec{k}$ , but if we go to large enough  $|\vec{k}|$  we can find values of  $\vec{k}$  for which  $|\vec{\omega} \cdot \vec{k}|$  becomes small. How small a value  $|\vec{\omega} \cdot \vec{k}|$  can be found as  $|\vec{k}|$  becomes large determines “how irrational” the frequency ratios are. KAM theory tells us that for  $\varepsilon \rightarrow 0$  and smooth enough perturbations the surviving irrational tori are the ones with  $\vec{\omega}_0$  satisfying

$$|\vec{\omega}_0 \cdot \vec{k}| > \gamma |k|^{-\tau} \quad (28.2)$$

for *all* vectors of integers  $\vec{k}$  and some  $\gamma$  and  $\tau$  with bounds placed on  $\tau$  that can be refined depending on smoothness conditions placed on the perturbation and restrictions on the unperturbed system. For example KAM showed that tori survive for  $C^r$  perturbations if  $N - 1 < \tau < \frac{1}{2}r - 1$  and  $\gamma$  is of order  $\sqrt{\varepsilon}$  for small  $\varepsilon$ . (There are in fact no  $\vec{\omega}_0$  satisfying the Diophantine condition with  $\tau < N - 1$ , for  $\tau = N - 1$  the  $\vec{\omega}_0$  are a set of measure zero, and so  $\tau > N - 1$  is the requirement for the survival of “most” tori. This then sets requirements on the smoothness of the perturbation  $r > 2N$ .)

The need for such conditions can be seen by delving a little into the perturbation theory for the system. In terms of the generating function method for canonical transformations we seek a function  $S(\vec{I}', \theta)$  where

$$\vec{I} = \frac{\partial S}{\partial \vec{\theta}}, \quad \vec{\theta}' = \frac{\partial S}{\partial \vec{I}'} \quad (28.3)$$

such that the transformed Hamiltonian is independent of  $\vec{\theta}'$

$$H'(\vec{I}') = H(\vec{I}, \vec{\theta}) = H\left(\frac{\partial S}{\partial \vec{\theta}}, \vec{\theta}\right). \quad (28.4)$$

We can expand  $S$

$$S(\vec{I}', \theta) = \vec{I}' \cdot \vec{\theta} + \varepsilon S_1(\vec{I}', \theta)$$

so that (28.4) becomes to first order in  $\varepsilon$

$$H'(\vec{I}') = H_0(\vec{I}') + \varepsilon \frac{\partial H_0(\vec{I}')}{\partial \vec{I}'} \cdot \frac{\partial S_1}{\partial \vec{\theta}} + \varepsilon H_1(\vec{I}', \theta). \quad (28.5)$$

If we now write the periodic  $\theta$  dependence of  $S_1$  and  $H_1$  in terms of their multidimensional Fourier series

$$S_1(\vec{I}', \theta) = \sum_m S_{1,m}(\vec{I}') e^{i\vec{m} \cdot \vec{\theta}} \quad \text{etc.} \quad (28.6)$$

and collect coefficient of each Fourier component we find

$$S_1(\vec{I}', \theta) = \sum_m \frac{H_{1,m}(\vec{I}')}{\vec{m} \cdot \vec{\omega}_0(\vec{I}')} e^{i\vec{m} \cdot \vec{\theta}}. \quad (28.7)$$

The difficulty is the “small denominators”  $\vec{m} \cdot \vec{\omega}_0(\vec{l}')$ : even for irrational frequency ratios, we can expect to find some  $\vec{m}$  if we go to large enough  $|\vec{m}|$  such that this denominator becomes very small. And the importance of the small denominators grows at higher orders in the perturbation series. The subtlety of KAM theory is controlling these divergences with the stated constraints on the sizes of the small denominators and the fall off of the  $H_{1,m}$  with large  $m$  depending on the smoothness of the perturbation.

## 28.2 Break down of the rational tori

The fate of the rational tori can be investigated using the Mosur twist map.

For the unperturbed system in action-angle coordinates the map  $M$  is

$$\begin{aligned} r_{n+1} &= r_n \\ \theta_{n+1} &= \theta_n + 2\pi a(r_n) \end{aligned} \tag{28.8}$$

where  $a(r) = \omega_1/\omega_2$  the ratio of the frequency of the map to the frequency eliminated in forming the Poincaré section. It is assumed  $da/dr \neq 0$ . For rational frequency ratios  $\omega_1/\omega_2 = p/q$  with  $p, q$  integers each point on the circle  $r = r_{pq}$  with  $a(r_{pq}) = p/q$  is a fixed point of the map iterated  $q$  times i.e.  $M^q$ .

Now perturb the twist map to  $M_\varepsilon$

$$\begin{aligned} r_{n+1} &= r_n + \varepsilon f(r_n, \theta_n) \\ \theta_{n+1} &= \theta_n + 2\pi a(r_n) + \varepsilon g(r_n, \theta_n) \end{aligned} \tag{28.9}$$

and consider the effect of  $M^q$  in the vicinity of  $r_{pq}$ . By continuity with the unperturbed case, for each  $\theta$  we can find a radius at which the point is mapped purely in the radial direction (i.e. zero twist). Connecting these points gives a continuous curve  $R_\varepsilon$  (the deformation of  $r = r_{pq}$ ) that is mapped only in the radial direction by  $M^q$ . By the area preserving property of the map the image  $M_\varepsilon^q R_\varepsilon$  of this curve under  $M_\varepsilon^q$  must intersect  $R_\varepsilon$  in an *even* number of points (see figure 28.1), and these are fixed points of  $M_\varepsilon^q$ . The sketch in figure 28.1 shows that these must be alternating elliptic and hyperbolic fixed points.

We next show that there in fact at least  $2q$  fixed points of  $M_\varepsilon^q$ . Let  $(r_0, \theta_0)$  be one of the fixed points. For the unperturbed map  $(r_0, \theta_0), M(r_0, \theta_0), \dots, M^{q-1}(r_0, \theta_0)$  are distinct points and for the perturbed system

$$M_\varepsilon^q M_\varepsilon(r_0, \theta_0) = M_\varepsilon(r_0, \theta_0) \tag{28.10}$$

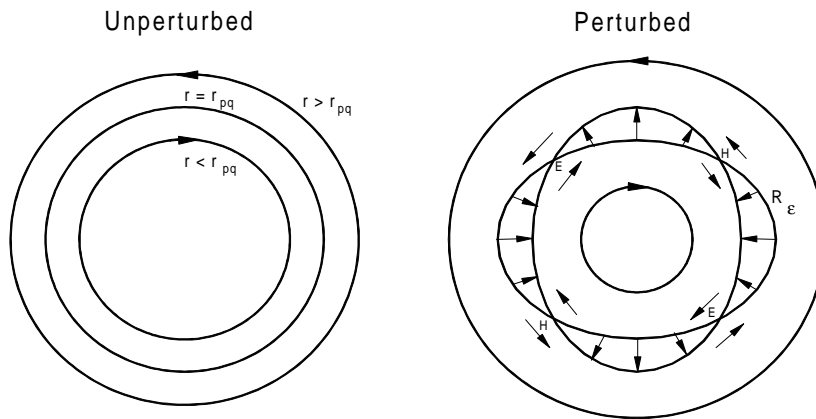


Figure 28.1: Behavior of the map  $M^q$  in the integrable and perturbed cases. For the unperturbed map there is a circle of fixed points at  $r = r_{pq}$ . In the perturbed case we can find a continuous curve  $R_\varepsilon$  that is mapped without twist (i.e. in the radial direction). The mapping  $M^q R_\varepsilon$  is shown by the arrows. There are an even number of intersections corresponding to alternating elliptic and hyperbolic fixed points, and can be seen combining the radial mapping with the twist that increases to larger  $r$ .

i.e.  $M_\varepsilon(r_0, \theta_0)$  is also a fixed point of  $M_\varepsilon^q$ . Therefore there are at least  $q$  distinct fixed points of  $M_\varepsilon$  on  $R_\varepsilon$ . But elliptic fixed points cannot be mapped into hyperbolic fixed points, so there must be  $2nq$  fixed points of  $M_\varepsilon^q$  (with  $n$  an integer) in the vicinity of  $r_{p,q}$ .

What is the behavior near the fixed points of  $M_\varepsilon^q$ ?

### 28.2.1 Behavior near elliptic fixed point

Near enough to the fixed point we would expect the twist map  $M$  to again describe the limit cycles around the fixed point. Now we get the same behavior! Sufficiently irrational circle survive; rational circles break up to a sequence of elliptic and hyperbolic fixed points etc. The same behavior is repeated on finer and finer scales.

### 28.2.2 Behavior near hyperbolic fixed point

The stable and unstable manifolds of the hyperbolic fixed points will typically intersect leading to homoclinic tangles which implies the existence of horseshoes and chaos (see [chapter 23](#)).

### 28.2.3 Period doubling bifurcations of the elliptic fixed points.

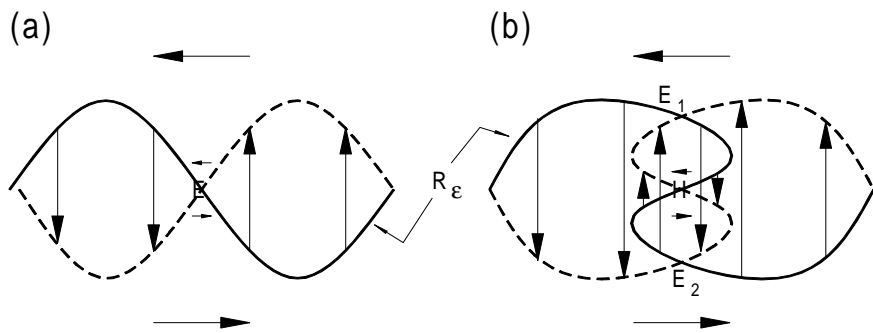


Figure 28.2: Period doubling instability of the elliptic fixed point. The continuous curve  $R_\epsilon$  is the curve  $R_\epsilon$  mapped by  $M^q$  with zero twist to the dashed curve. In (a) this gives the elliptic fixed point  $E$ . In (b) the curve  $R_\epsilon$  has become sufficiently distorted to give two new intersections with  $M^q R_\epsilon$  i.e. the points  $E_1$  and  $E_2$ . The arrows denoting the mapping show that  $E_1$  and  $E_2$  are mapped into each other, and the fixed point  $H$  is now hyperbolic with reflection. Under  $M^{2q}$   $E_{1,2}$  are elliptic fixed points.

As the nonlinearity increases the elliptic fixed points can themselves become unstable undergoing an infinite sequence of period doubling bifurcations to chaos. The geometry of these transitions is sketched in figure (28.2). In panel (b)  $E_1$  and  $E_2$  are mapped into each other by  $M^q$ , and the elliptic fixed point has become hyperbolic. Under  $M^{2q}$  the points  $E_1$  and  $E_2$  are elliptic fixed points, and the same behavior can be repeated. A fascinating aspect of these period doubling transitions is that because of the constraint of area preserving the transition belongs to a different universality class than the quadratic map, with  $\delta = 8.721\dots$  and  $|\alpha| = 4.018\dots$  (see for example Schuster's book, Appendix G).

### 28.2.4 Breakup of the last KAM torus

For a 2-d map the KAM tori divide the phase space into disjoint regions: chaotic motion starting from an initial condition within the torus cannot escape through the torus. This result is not entirely obvious: since we are dealing with discrete iterations it might seem possible that the orbit could “hop across” the invariant torus. However considering the mapping of the area inside the torus as a whole, and the constraint of area preserving, is enough to prove the result.

For the standard map the tori for  $K = 0$  span the range  $0 < x \leq 1$  and divide the  $y$  range into stripes. As the tori are successively destroyed as  $K$  increases these regions connect, but until the last surviving torus disappears the chaotic motion is confined to a limited range of  $y$  bracketing the initial condition. For this map the last surviving torus is the one with winding number the Golden Mean  $\frac{1}{2}(\sqrt{5} - 1)$ , and the “crinkling” of the smooth curve at the breakdown point  $K = K_c \simeq 0.97$  has interesting scaling properties [1].

### 28.2.5 Arnold Diffusion

In two dimensions after the break up of the last torus, or in higher dimensions where the surviving tori are not sufficient to confine the motion even for arbitrarily small nonintegrable perturbation, a chaotic trajectory will eventually tend to wander to distant regions of phase space. For example in the periodically kicked rotor the kinetic energy will eventually become large. This process is known as Arnold diffusion.

The diffusive nature of the process is easily seen for the standard map at large  $K$ . Here we have

$$\Delta y_{n+1} = y_{n+1} - y_n = -\frac{K}{2\pi} \sin 2\pi x_n \quad (28.11)$$

and  $x_{n+1} - x_n$  will be large so that  $x_n \bmod 1$  will vary wildly. We might then take  $\sin 2\pi x_n$  to be a random variable in the range between  $\pm 1$  so that  $y_n$  evolves as a random walk

$$\langle y_n^2 \rangle \sim n \left( \frac{K}{2\pi} \right)^2 \langle \sin^2 2\pi x_n \rangle \quad (28.12)$$

i.e. diffuses with a diffusion constant  $D = \frac{1}{2}(K/2\pi)^2$ . For smaller  $K$ , approaching the critical value  $K_c$ , or for weak nonintegrability in higher dimensions, the diffusion will become much slower.

## 28.3 Strong Chaos

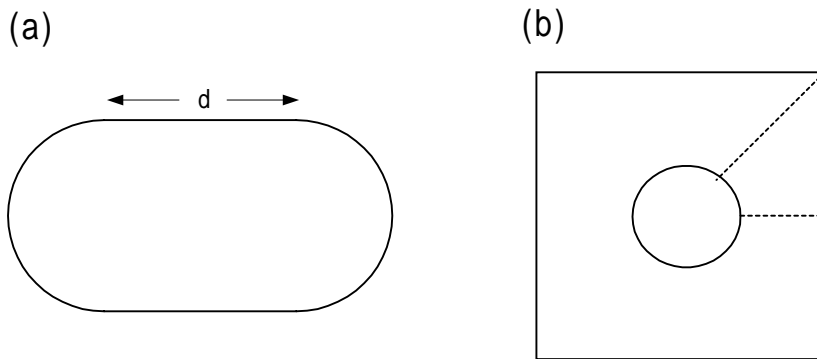


Figure 28.3: Ergodic and mixing chaotic systems: (a) particle in stadium; (b) Sinai billiards. In the later case taking the small segment marked with dotted lines eliminates the reflection symmetries.

Even after the last KAM surface has broken down in the circle map, there are still invariant curves enclosing regions of phase space, and the system is still not ergodic—not all initial conditions (except for a set of measure zero) lead to orbits that visit all regions of phase space consistent with the conserved quantities. Since ergodicity is a key assumption of statistical mechanics (albeit at large phase space dimensions) it is interesting to construct simple dynamical systems that are ergodic and also mixing. The latter property ensures that correlation functions relax to the “equilibrium” values given by averages over the available phase space. The two systems consisting of a particle bouncing between the walls shown in figure 28.3 are chaotic, ergodic and mixing. The stadium shown in (a) is chaotic for all non-zero values of the straight edge length  $d$ ; of course it is integrable for  $d = 0$ .

*December 17, 1999*

# Bibliography

- [1] L.P. Kadanoff, Phys. Rev. Lett. **47**, 1641 (1981)